DOI: 10.1534/genetics.107.078626

aubergine Gene Overexpression in Somatic Tissues of *aubergine*^{sting} Mutants Interferes With the RNAi Pathway of a *yellow* Hairpin dsRNA in *Drosophila melanogaster*

Valeria Specchia,* Clara Benna,† Gabriella Margherita Mazzotta,† Alberto Piccin,†,[1] Mauro A. Zordan,† Rodolfo Costa† and Maria Pia Bozzetti*,[2]

**Dipartimento di Scienze e Tecnologie Biologiche ed Ambientali, Università del Salento, 73100 Lecce, Italy and* †*Dipartimento di Biologia, Università di Padova, 35121 Padova, Italy*

Manuscript received July 10, 2007
Accepted for publication January 9, 2008

ABSTRACT

AUBERGINE (AUB) is a member of the PPD family of proteins. These proteins are implicated in RNA interference. In this article we demonstrate that the expression of the *aub* gene and protein increase in *aub*^{sting} mutants. We used a genetic method to test whether *aub*^{sting} overexpression could interfere with proper functioning of the process of RNA interference in somatic tissues of *Drosophila melanogaster*. This method is based on a transgenic line bearing a construct in which a fragment of the *yellow* (*y*) gene is cloned to form an inverted repeat (*y-IR*) under the control of the upstream activation sequence (*UAS*) of the yeast transcriptional activator GAL4. The *UAS-y-IR* transgene and the *Act5C-GAL4* driver were brought together on chromosome 3 via recombination. In the resulting strain (*Act5C-y-IR*), transcriptional activation by GAL4 constitutively produces a dsRNA hairpin bearing cognate sequences to the *yellow* gene causing continuing degradation of *y* mRNA resulting in *yellow*^{1} (*y*^{1}) phenocopies. In this genetic background, the mutation of any factor involved in RNAi should repress degradation of *y* mRNA, restoring the wild-type phenotype. We employed this genetic approach to show that an increased amount of AUBERGINE interferes with the regular functioning of the somatic RNAi pathway.

RNA interference (RNAi) is a widespread homology-dependent silencing mechanism mediated by double-stranded RNA (dsRNA). RNAi-mediated gene silencing suppresses gene expression by several mechanisms, including the targeted sequence-specific cleavage of mRNA, translational repression, and the maintenance of silenced regions of chromatin (reviewed in Jaronczyk *et al.* 2005; Kavi *et al.* 2005; Cerutti and Casas-Mollano 2006; Valencia-Sanchez *et al.* 2006; and references therein). RNAi is also known to influence many biological processes such as heterochromatin formation, post-transcriptional gene regulation during development, DNA elimination, cell-cycle regulation, RNA editing, and mRNA decay (Pal-Bhadra *et al.* 2004; Matzke and Birchler 2005; Tomari and Zamore 2005; Lee and Collins 2006; and references therein). RNAi has probably evolved as a genome "immunity" system to protect the integrity of eukaryotic genomes and maintain chromosome stability through avoiding invasion by exogenous nucleic acids introduced by mobile genetic elements such as viruses and transposons.

Different classes of small RNA molecules 19–31 nt in length have been identified as sequence-specific regulators for diverse RNAi pathways; they have been classified in small interfering RNAs (siRNAs), microRNAs (miRNAs), repeat-associated small interfering RNAs (rasiRNAs), and the recently identified Piwi-associated interfering RNAs (piRNAs) (Carthew 2006; Kim 2006; Watanabe *et al.* 2006; Brennecke *et al.* 2007; Lin 2007; and references therein). Both siRNAs and miRNAs are 21–23 nt long and they are incorporated into related RNA-induced silencing complexes (RISCs), which are referred to as siRISC and miRISC. They are responsible for post-transcriptional gene silencing either by driving the cleavage of homologous mRNAs (siRNAs) or by blocking translation following binding to the 3′-UTR of homologous mRNAs (miRNAs), depending on the extent of pairing (Hutvagner and Zamore 2002; Doench *et al.* 2003; Zeng *et al.* 2003; Tang 2005). rasiRNAs (24–26 nt) arise from genomic repeated regions and they are presumably implicated in chromatin modifications at these sites (Aravin *et al.* 2003; Pal-Bhadra *et al.* 2004; Vagin *et al.* 2004, 2006; Gunawardane *et al.* 2007). piRNAs (26–31 nt) have been recently isolated from rat, mouse, Drosophila, and human male germ tissues (Carthew 2006; Grivna *et al.* 2006; Kim 2006; Watanabe *et al.* 2006; Brennecke *et al.* 2007).

[1]Deceased.

[2]*Corresponding author:* Dipartimento di Scienze e Tecnologie Biologiche ed Ambientali Università del Salento, Ekotekne-Via per Monteroni, 73100 Lecce, Italy. E-mail: maria.bozzetti@unile.it

Biochemical dissection of the RNAi pathway in animals has revealed that RNaseIII-like enzymes named Dicer are required for dicing the dsRNA molecule into small RNAs, which trigger RNAi pathways (Pham and Sontheimer 2005; Tomari and Zamore 2005; Vaucheret 2006). While only a single Dicer protein is present in mammals, in *Drosophila melanogaster*, siRNAs and miRNAs are produced by distinct Dicer enzymes: Dicer-2 is involved in the production of siRNAs, starting from either dsRNAs or from short hairpin RNAs (shRNAs) resulting from RNA polymerase II transcripts of inverted repeat-bearing artificial constructs (Kennerdell and Carthew 2000; Lee *et al.* 2004; Pham *et al.* 2004; Tomari and Zamore 2005); Dicer-1 is required for the processing of pre-microRNA stem-loop dsRNAs into microRNAs (Lee *et al.* 2004). Small RNAs, generated by Dicer, are loaded onto RISCs where their unwinding takes place. In the Argonaute (Ago) family of proteins two distinct RNA-binding domains, PAZ and PIWI domains (PPD) (Cerutti *et al.* 2000; Hammond *et al.* 2001; Catalanotto *et al.* 2002; Morel *et al.* 2002; Denli and Hannon 2003; Lee *et al.* 2004), are required to bind the siRNA and to slice the cognate RNA to be degraded, respectively (reviewed in Collins and Cheng 2005; Lingel and Sattler 2005). Members of the Ago or PPD family of proteins are key components of RISC (Liu *et al.* 2004; Meister *et al.* 2004; Song *et al.* 2004). Most organisms have multiple members of the Ago proteins; for example, humans have 8 different Ago proteins, *Caenorhabditis elegans* has 27, and *Schizosaccharomyces pombe* has only 1. It has been demonstrated that these proteins are specialized for different functions (Hammond *et al.* 2001; Caudy *et al.* 2002; Ishizuka *et al.* 2002; Mourelatos *et al.* 2002; Denli and Hannon 2003; Liu *et al.* 2003; Verdel *et al.* 2004; Yigit *et al.* 2006; Brennecke *et al.* 2007). Thus, Argonaute proteins can be grouped into Ago and Piwi subclasses: the Ago members, which are expressed ubiquitously and associated with siRNAs and miRNAs and the Piwi members, which are preferentially expressed in germ-line and stem cells (Aravin *et al.* 2006; Girard *et al.* 2006; Grivna *et al.* 2006; Watanabe *et al.* 2006). In *D. melanogaster* five members of the PPD proteins have been identified: AGO1 and AGO2, which belong to the Ago subfamily; AGO3, PIWI, and AUBERGINE (AUB), which belong to the Piwi family (Cox *et al.* 1998; Schmidt *et al.* 1999; Williams and Rubin 2002). For some of them a role in RNAi has been demonstrated: AGO1 and AGO2 are associated with RISC (Hammond *et al.* 2001; Carmell *et al.* 2002; Williams and Rubin 2002; Meister and Tuschl 2004; Okamura *et al.* 2004; Tomari *et al.* 2004); AGO3 binds the piRNAs (Brennecke *et al.* 2007); PIWI is implicated in RNAi-related mechanisms affecting both transcriptional and post-transcriptional transgene silencing (PTGS and TGS) (Pal-Bhadra *et al.* 2002) and in the rasiRNA-derived pathway (Pelisson *et al.* 2007); and AUB has been demonstrated to be required in RISC assembly *in vitro* (Tomari *et al.* 2004) and in RNAi in oocytes *in vivo* (Kennerdell *et al.* 2002). AUB is a polar granule component required for pole cell formation (Harris and Macdonald 2001) and it is genetically involved in two processes: the translational regulation of *oskar* and *gurken* mRNAs and the localization of *nanos* mRNA (Wilson *et al.* 1996; Harris and Macdonald 2001; Cook *et al.* 2004).

The *aub* gene was first described as being involved in the determination of both the dorsoventral and anteroposterior embryonic patterns during Drosophila development (Schüpbach and Wieschaus 1991; St Johnston and Nüsslein-Volhard 1992; Wilson *et al.* 1996). *sting* was identified in a screen for male-sterility mutants following random insertional mutagenesis with a *P* (*lacW*) element (Bier *et al.* 1989). Originally, the gene affected by the *sting* mutation was demonstrated to be a modifier of the *crystal-Stellate* system (Schmidt *et al.* 1999; Tritto *et al.* 2003) and was named *sting* (***St****ellate* **in**teracting **g**ene). Later, *sting* was determined to be an allele of *aubergine* (Harris and Macdonald 2001). The name of this allele was thus changed to *aubergine*^{sting} (*aub*^{sting}).

aub^{sting} is not a "loss-of-function mutation" because its transcript is produced but it is not properly regulated in both sexes (Schmidt *et al.* 1999). In the testes of homozygous *aub*^{sting} males, STELLATE crystalline aggregates form, the morphology of which depends on the number of the X-linked *Stellate* repeats; such males also exhibit meiotic defects in chromosome condensation and segregation. This behavior overlaps the phenotype resulting from a deletion of *crystal* (Schmidt *et al.* 1999; Tritto *et al.* 2003). The *crystal-Stellate* system represents the first case of "natural dsRNA-mediated silencing"; in fact, in wild-type testes the production of STELLATE protein, the main component of crystals in the spermatocytes of *aub*^{sting} mutants, is prevented by the degradation of *Stellate* mRNA, accompanied by the production of 25–27 nt siRNAs (Aravin *et al.* 2001). In X/Y*cry*$^{-}$ males no such siRNAs are found, and *Stellate* mRNA is translated, leading to the production of STELLATE protein and the formation of crystalline aggregates in spermatocytes. In addition, five different *Stellate/crystal* homologous rasiRNAs have been identified in X/Y male testes (Aravin *et al.* 2003).

Our present understanding of dsRNAi has so far relied on the identification and characterization of numerous molecules involved in different RNAi pathways (Kim 2006; Saito *et al.* 2006; Vagin *et al.* 2006; Watanabe *et al.* 2006; Pelisson *et al.* 2007). In the present study we demonstrated that the *aubergine*^{sting} (*aub*^{sting}) mutation produces an increased transcription of the *aub* gene leading to overexpression of the AUB protein in somatic tissues. The subsequent analysis of the RNAi triggered by a *yellow* hairpin dsRNA revealed that the gene silencing was impaired in *aub*^{sting} mutants, suggesting that the overexpression of AUB protein interferes with some crucial component or function of the RNAi pathway in somatic tissues.

MATERIALS AND METHODS

Fly stocks: The *aubergine*^{sting} *P*-insertion line (Bier *et al.* 1989; Schmidt *et al.* 1999) was kept over the *CyO* balancer chromosome (Lindsley and Zimm 1992) and made homozygous when required in backcrosses throughout the experiments described below. We also used two different *aubergine* alleles that we ordered from the Bloomington Stock Center: *aub*[HN] *cn*[1] *bw*[1]/*CyO* (BL-8517) and *w*[1118]; *aub*[*QC42*] *cn*[1] *bw*[1]/*CyO*, P{ry[+t7.2] = sevRas1.V12}FK1 (BL-4968). In addition we used the strain called *UAS-aub*, kindly provided by M. Snee from the laboratory of Paul Macdonald. It is a transgenic fly strain *UAS-GFP-aub* (Harris and Macdonald 2001).

The *UAS-y-IR* 5F transgenic line has already been described (Piccin *et al.* 2001). It is homozygous for the *UAS-y-IR* transgene (single copy) which has been mapped to 3R 98–99. The transgenic line *Act5C-GAL4/TM6B, Tb* was obtained from the Bloomington Stock Center (strain 3954, *y, w; P{w+; Act5C-GAL4}17bFO1/TM6B, Tb*). Individuals from this line produce GAL4 constitutively under the control of an *actin* promoter. *Sco/CyO; MKRS/TM6B* is a compound strain with balancers for the two main autosomes carrying dominant mutations; the *Sco* chromosome present in this strain is Tp(2;2) noc^{Sco} (Lindsley and Zimm 1992). *w/w; Apt/TM6B* is a strain used in the procedure adopted to set up the fly stock bearing the *Act5C-GAL4* and *UAS-y-IR* constructs in association with the third chromosome. Flies were raised on a standard yeast–glucose–agar medium (Roberts and Standen 1998) and were maintained at 25°, 70% relative humidity, in 12-hr light/12-hr dark cycles.

Construction of the fly stock bearing the *Act5C-GAL4* and *UAS-y-IR* constructs on the third chromosome: We used transgenic line 5F (which is homozygous for the *UAS-y-IR* construct) and the transgenic *Act5C-GAL4/TM6C, Tb* "driver" line expressing GAL4 under the control of the *Actin5C* promoter (Piccin *et al.* 2001). Using a number of crosses, we generated the *w/w/Y; Act5C-y-IR/TM6B* line, which, due to constitutive expression of the *UAS-y-IR* transgene, generates yellow male and female phenocopies.

Microscopy and images: Phenotypes were scored using a Nikon stereomicroscope; images were collected using a Nikon digital camera mounted on a Leica stereomicroscope.

Total RNA extraction: Total RNA was extracted from 30 mg of adults (~30 females and 40 males deprived of gonads) using RNeasy mini kit (QIAGEN, Valencia, CA) reagent following the manufacturer's protocol. The RNA concentration and purity were determined photometrically by measuring absorbance at 260 nm and A260/A280 ratio. Samples were then dissolved in 15 μl of mix (470 μl deionized formamide, 157 μl 37% formaldehyde, 98 μl 10× MOPS, 275 μl sterile water) and heated at 60° for 15 min. Two microliters of RNA loading buffer were added to each sample. Electrophoresis was performed on a 1% agarose MOPS formaldehyde gel as described in (Sambrook *et al.* 1989).

Northern blot analysis: After electrophoresis the formaldehyde–agarose gel was photographed and washed in sterile water for 10 min and then in 20× SSC for 1 hr. Transfer was performed on a Hybond N membrane (Amersham, Piscataway, NJ) overnight. Baking was for 45 min at 80° under vacuum. Hybridization was performed in 25 ml of 5× SSPE/5× Denhardt's/0.5% SDS/herring sperm DNA (100 μg/ml) at 68° overnight. After hybridization, the filter was washed at 68° for 5 min in 2× SSC/0.1% SDS twice and then in 1× SSC/0.1% SDS for 15 min. Autoradiography was performed using Kodak film.

Probes amplification and cloning: A 1143-bp coding fragment from *yellow* cDNA, amplified with upper primer 5′ CTTGACTTGACCAGCCATAC 3′ (with the *Xba*I site at the 5′ end of the primer) and lower primer 5′ ATGATGCCACCACC CAGATTG 3′ (with the *Hin*dIII site at the 5′ end of the primer) was obtained by RT–PCR; afterward it was inserted in the pGEM7 vector. The *yellow* fragment was excised by *Xba*I–*Hin*dIII restriction enzymes and labeled with standard random priming procedure using 5 μl of ^{32}P-dATP (3000 Ci/mmol).

For normalization of the RNA amount we used the 28S RNA. We synthesized the first strand, from total RNA extracted from adults, using a 28S rRNA RT–PCR lower primer 5′ ATAAAA CAGAAAAGAAAACT 3′ and the SuperScript II RNaseH-reverse transcriptase (Invitrogen, Carlsbad, CA). Afterward we amplified adding the upper primer 5′ TAAAACAGCAGGACG GTGAT 3′. The PCR profile consisted of a denaturation step (94°, 10 min) followed by 40 cycles (94° 1 min; 50° 1 min; 72° 1 min); for the last cycle only the elongation step (72°) was extended to 10 min. The 500-bp fragment was then labeled with standard random priming procedure using 2 μl of ^{32}P-dATP (SA 3000 Ci/mmol).

cDNA synthesis from total RNA: Total RNA was extracted, as described before. To remove all the DNA in the preparation, the samples were incubated with DNase I RNase free (Roche, Indianapolis) (1 unit/μg RNA) at 37° for 10 min, in a total volume of 100 μl. After treatment DNase was inactivated at 75° for 10 min. DNase treated RNA was precipitated at −80° overnight and it was dissolved in 30 μl of distilled water. For first-strand cDNA synthesis, 5 μg of total RNA was used as a template for oligonucleotides dT(17) primed reverse transcription using SuperScript II RNaseH-reverse transcriptase (Invitrogen), according to the manufacturer's instructions.

Quantitative real-time PCR: Real-time RT–PCR was performed in the SmartCycler real-time PCR (Cepheid, Sunnyvale, CA). Relative abundance of the *yellow* and *aubergine* transcripts was determined by real-time PCR using Fluo cycle for SYBR Green (Celbio) according to the manufacturer's protocol. For quantification of the *yellow* transcripts we used the standard curve method as described in (Ponchel *et al.* 2003; Larionov *et al.* 2005) whereas we used the 2ΔΔct method (Livak and Schmittingen 2001) for the *aubergine* transcript determination. The primers for *yellow* transcript were *yellow* upper 5′ GTGTGATGAGCGATGATGGA 3′ and *yellow* lower 5′ GCAAGAAAACGGGCATCCTA 3′; the primers for *rp49* transcript were *rp49* upper 5′ ATCGGTTACGGATC GAACAA 3′ and rp49 lower 5′ GACAATCTCCTTGCGCTTCT 3′ (for the standard curve of *rp49* we used a clone kindly provided by Maria Berloco from the Genetics laboratory (University of Bari, Bari, Italy); the clone has a 700-bp *Eco*RI–*Hin*dIII coding fragment from *rp49* cDNA inserted in the *Eco*RI–*Hin*dIII site of pUC vector); and the primers for the *aub* transcript were *aubergine* upper 5′ CGTGGTCGAGGAAGAAA GCC 3′ and *aubergine* lower 5′ CCCACTTGAGCATCACCACC 3′ [for the standard curve of *aubergine* we used the amplicon obtained by RT–PCR using the described primers; to be sure that it was the specific product of the *aub* gene we sequenced it; in addition we determined the melting temperature (T_m) of the amplicon]. PCR amplification was performed in a final volume of 25 μl using standard cycling parameters [10 min, 95°; 30 sec, 95°; 30 sec, 53° (*yellow*), 56° (*rp49*) and 60° (*aubergine*); 30 sec, 72° with the latter three steps repeated 45 times]. For each sample we calculated the amplification efficiency $E = [10^{-1/\text{slope}}] - 1$ and the melting curve to ensure that the desired amplicon was detected. The efficiencies of amplification of the target genes and the control were approximately the same.

In the standard curve method, the sample amount was calculated as follows: sample [pg] = $10^{(\text{ct sample} - \text{intercept})/\text{slope}}$. Normalization for each determination was obtained by dividing each quantitative value calculated for *yellow* by the quantitative value of the *rp49* gene, in experimental samples. For all the genotypes we also calculated the coefficient of variation (CV)

as standard deviation/mean value. Afterward, value 1 was assigned to the *yellow* relative amount with respect to the *rp49* amount in the control genotype (aub^{sting}/aub^{sting}) and the fold change for each analyzed genotype was calculated. The error of the relative amount of *yellow/rp49* was calculated as CV with this formula: $CV = \sqrt{cv^2_{sample} + cv^2_{control}}$; the standard deviation shown on the graph was calculated as standard deviation = CV × mean value.

In the 2ΔΔct method, the relative amount of *aub* transcript (fold change) was calculated as follows: $X\,\text{test}/X\,\text{control} = 2^{\Delta\Delta ct} = 2^{(Ct_X - Ct_R)}\text{control}^{-(Ct_X - Ct_R)}\text{test}$ [Ct_X is Ct of gene of interest (*aub*) and Ct_R is Ct of reference gene (*rp49*); test refers to the different cDNAs to analyze and control refers to the cDNA of reference (wild type)]. The error was calculated as $CV = \sqrt{cv^2_{test,X} + cv^2_{test,R}}$.

Protein extraction and Western blotting: Protein samples were prepared from dissected tissues (40 mg) by squashing them and extracting the proteins in lysis buffer (6% SDS, 1 mM EDTA, 0.2 mM PMFS).

Samples were denatured in single-strength sample buffer [10 mM Tris/HCl, pH 8, 1 mM EDTA, 10% (v/v) glycerol, 2% (w/v) SDS, 5% (v/v) β-mercaptoethanol and 0.001% (w/v) bromophenol blue], heated for 5 min at 100°, and subjected to SDS–PAGE in minislab gel containing 10% acrylamide and 0.10% bisacrylamide. Molecular-weight markers were run to estimate the molecular weight of the immunoreactive band. After electrophoresis, the proteins were transferred electrophoretically (100 V for 1 hr) to a sheet of nitrocellulose using the mini Bio-Rad trans blot apparatus and 20 mM Tris, 150 mM glycine, 20% (v/v) methanol at pH 8.2 as transfer buffer. After protein transfer, the nitrocellulose sheet was incubated with 3% BSA (w/v) in 10 mM Tris/HCl pH 7.5, 150 mM NaCl and hybridized with anti-AUB/STING antibody, a rabbit polyclonal antiserum, ab17724 (Abcam, Cambridge, MA), diluted 1:500 in TNT buffer (10 mM Tris/HCl, pH 7.5, 150 mM NaCl, 0.5% Triton X-100). This antibody was raised against a 20-amino-acid peptide located at the C-terminal of the AUBERGINE protein (Abcam, C. Wong, personal communication). This peptide is specific for the AUBERGINE protein and no similarities have been found with any of the other PPD Drosophila proteins. Hybridization was performed overnight at room temperature. After washing, a peroxidase-conjugated donkey antirabbit IgG (Amersham) 1:2500 diluted in TNT buffer was used as the substrate for the colorimetric peroxidase reaction.

RESULTS

The *aubergine* gene is overexpressed in somatic tissues of aub^{sting} mutants: In a previous analysis by Northern blot, reported in Schmidt *et al.* (1999), we demonstrated that the expression of *aub* occurs prevalently in germ tissues. To quantify the amount of *aub* transcript in somatic tissues of homozygotes aub^{sting}/aub^{sting} compared to the heterozygotes and to the wild-type individuals, we performed quantitative real-time PCR starting from RNA extracted from males and females deprived of gonads. The T_m of the amplified fragment confirmed the specificity of the *aub* amplicon. We calculated the relative amount of *aub* transcript compared to *rp49* transcript in the genotypes of interest using the 2ΔΔct method described in materials and methods. Our results show that in wild-type (+/+) male somatic tissues the *aub* gene transcription takes place but it is improperly upregulated in both aub^{sting}/aub^{sting} and in aub^{sting}/CyO male somatic tissues (supplemental Table 1 and Figure 1A, bars 2 and 3) compared to wild type (Figure 1A, bar 1). Similar results were obtained in female somatic tissues (supplemental Table 2 and Figure 1C) even if the basal *aub* gene transcription in wild-type (+/+) gonadless female carcasses is slightly more abundant than in wild-type (+/+) gonadless male carcasses and the increase of the *aub* gene transcript is reduced in gonadless female carcasses (Figure 1C) compared to gonadless male carcasses (Figure 1A). We also estimated the amount of AUB protein in aub^{sting}/aub^{sting} and in aub^{sting}/CyO male mutants by Western blot. Drosophila AUB antiserum was a commercial antibody specific to the AUB protein (see materials and methods). It recognizes an ~97- to 98-kDa band as expected (Figure 2). We demonstrate that there is an evident increase of AUB protein in aub^{sting}/aub^{sting} and in aub^{sting}/CyO gonadless male carcasses compared to the control (Figure 2B, sections 2, 3, and 1, respectively), as expected by the transcriptional analysis reported before. These results are confirmed by the densitometric analysis reported in Figure 2C where a 3.5-fold increment in the aub^{sting}/aub^{sting} (Figure 2C, bar 2) and a 1.5-fold increment in aub^{sting}/CyO (Figure 2C, bar 3) with respect to wild type (Figure 2C, bar 1), is shown. All the densitometric values are reported in supplemental Table 3. We made three different Western blot experiments and we obtained the same results (data not shown).

aub^{sting} homozygous flies bearing the *Act5C-y-IR* chromosome exhibit a yellow$^+$ phenotype: We employed an *UAS-y-IR* transgenic line previously obtained in our laboratory causing heritable functional knockdown of an adult phenotype by the *in vivo* GAL4-driven production of a *yellow*-specific hairpin dsRNA. In particular, the *UAS-y-IR* construct consists of two inverted portions of the *yellow* gene, spaced by a heterologous sequence, placed under the control of a UAS domain. We previously showed that the progeny of crosses between flies harboring this transgene and flies expressing different GAL4 drivers, such as *daughterless* (*da-GAL4*) and *actin* (*Act5C-GAL4*), produced perfect yellow^2 and yellow^1 phenocopies, respectively (Piccin *et al.* 2001). A stable strain, bearing *Act-Gal4* and *UAS-y-IR* on the third chromosome was obtained by recombination. In this transgenic line, named *Act5C-y-IR*, transcriptional activation by Gal4 constitutively produces a dsRNA hairpin bearing cognate sequences to the *yellow* gene (*y*), which causes continuing degradation of *y* mRNA and the flies are therefore yellow^1 (y^1) phenocopies (Piccin *et al.* 2001).

We decided to use this "tester" genetic background to evaluate whether the $aubergine^{sting}$ mutation affects the degradation of *y* mRNA, thus restoring the wild-type phenotype. We employed dominant markers on chromosomes 2 and 3 to distinguish, among the progeny bearing the *Act5C-y-IR* constructs, flies that were homozygous

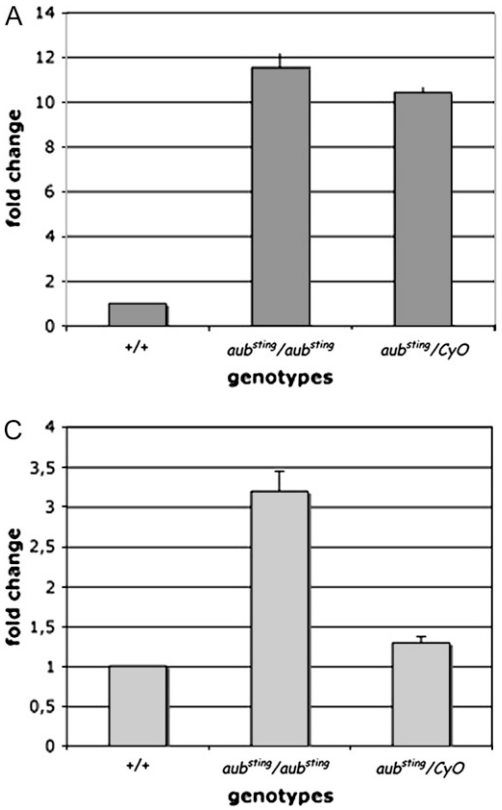

FIGURE 1.—Real-time PCR of *aub* transcript. Relative amounts of *aub* transcript respect to *rp49* in total RNA from gonadless carcasses are expressed on an arbitrary scale described in the text. (A) Bar 1, males +/+; bar 2, males *aub*^{sting}/*aub*^{sting}; bar 3, males *aub*^{sting}/*CyO*. (B) Fold change of *aub* transcript of the same genotypes reported in A *vs.* +/+. (C) Bar 1, females +/+; bar 2, females *aub*^{sting}/*aub*^{sting}; bar 3, females *aub*^{sting}/*CyO*. (D) Fold change of *aub* transcript of the same genotypes reported in C *vs.* +/+.

from those that were heterozygous for *aubergine*^{sting}. In this experiment we used the *Sco/CyO; MKRS/TM6B* strain to introduce dominant markers on chromosome 3 of the *aub*^{sting} strain and on chromosome 2 of the *Act5C-y-IR* strain; at first we crossed *aub*^{sting}/*CyO*; *TM6B* males with +/*Sco; Act5C-y-IR/MKRS* females; we recovered *aub*^{sting}/*Sco*; *Act5C-y-IR/TM6B* males and *aub*^{sting}/*Sco*; *Act5C-y-IR/TM6B* females to be crossed.

From this cross we selected 100 individuals that were homozygous and heterozygous for *aub*^{sting} and carried the *Act5C-y-IR* chromosome (since homozygosis for *Sco* and for *Act5C-y-IR* chromosome results in lethality, only *aub*^{sting}/ *aub*^{sting}; *Act5C-y-IR/ TM6B* and *aub*^{sting}/ *Sco; Act5C-y-IR/ TM6B* genotypes are present). All the individuals that were phenotypically Sco showed a yellow-like phenotype, whereas all the individuals that were phenotypically Sco^{+} were also phenotypically yellow^{+}. Chromosome-specific dominant markers allowed us to confirm that the wild-type (yellow^{+}) progeny, bearing the *Act5C-y-IR* construct, were also *aub*^{sting} homozygous. In Figure 3 all

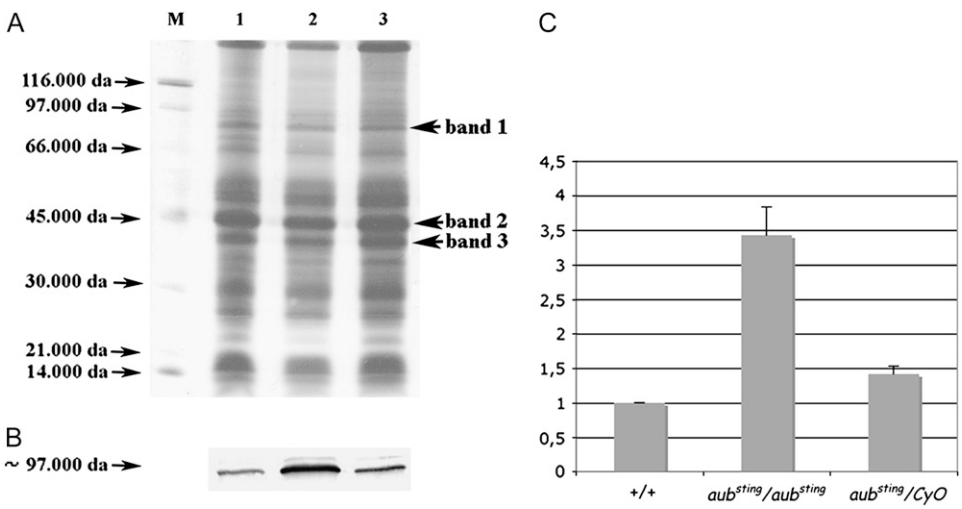

FIGURE 2.—(A) Gel electrophoresis stained with Blue Comassie of proteins extracted from 40 mg of gonadless male carcasses from different genotypes. M, marker; lane 1, +/+; lane 2, *aub*^{sting}/*aub*^{sting}; lane 3, *aub*^{sting}/*CyO*. (B) Western blot of gel reported in A, stained with an anti-AUBERGINE antibody. (C) Graph showing the densitometric analysis of the relative amount of AUB protein in Figure 2B (measured as OD × millimeters × millimeters) with respect to three different bands of proteins (marked with arrows) selected as controls. The arbitrary value of 1 was assigned to wild-type males. Bar 1, gonadless male carcasses +/+; bar 2, gonadless male carcasses *aub*^{sting}/*aub*^{sting}; bar 3, gonadless male carcasses *aub*^{sting}/*CyO*. The densitometric values are reported in supplemental Table 3.

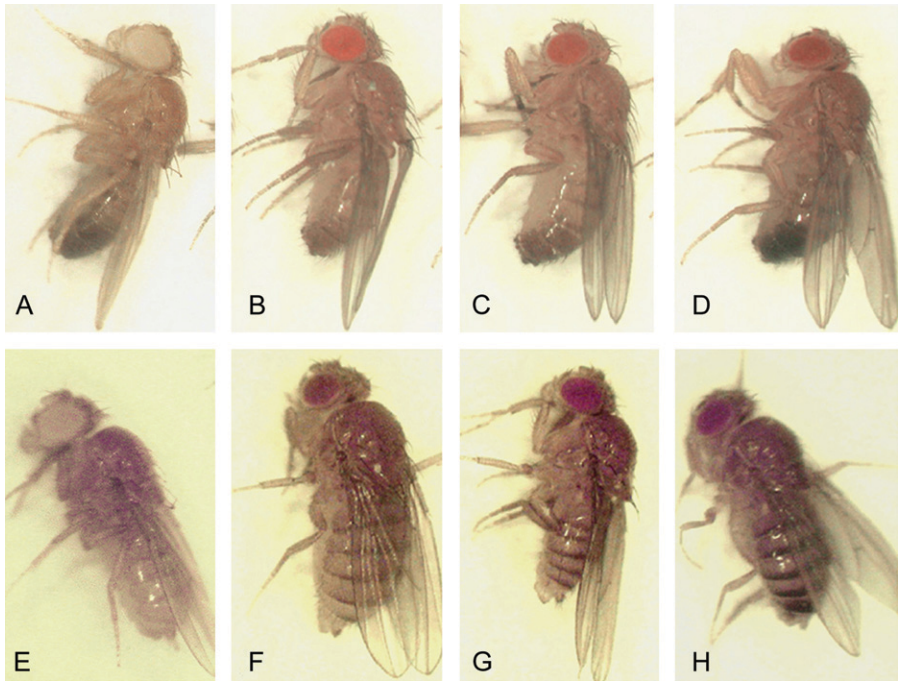

FIGURE 3.—Phenotypes observed in the progeny of crosses described in the text. (A) *yellow*^{1} hemizygous male; (B) male bearing the *Act5C-y-IR* construct (yellow); (C) heterozygous *aub*^{sting} male bearing the *Act5C-y-IR* construct; (D) homozygous *aub*^{sting} male bearing the same *Act5C-y-IR* construct (yellow^{+}) (E) *yellow*^{1} homozygous female; (F) female bearing the *Act5C-y-IR* construct (yellow); (G) heterozygous *aub*^{sting} female bearing the *Act5C-y-IR* construct; and (H) homozygous *aub*^{sting} female bearing the same *Act5C-y-IR* construct (yellow^{+}).

the individuals with the different genotypes examined are represented. Unlike males bearing the *Act5C-y-IR* construct (Figure 3B), which are very similar to *yellow*^{1} males (Figure 3A), *aub*^{sting} heterozygous males [showing the Scutoid (Sco) phenotype], which are characterized by the loss of 10–15 sternal bristles (LINDSLEY and ZIMM 1992), have a yellow-like phenotype (Figure 3C), even if it is less evident than in the +/+ males bearing the *Act5C-y-IR* construct. In contrast the *aub*^{sting}/*aub*^{sting} homozygous males showed wild-type (yellow^{+}) pigmentation (Figure 3D). In females the difference between *aub*^{sting} heterozygous and homozygous individuals is not so clear (Figure 3, G and H). This could be explained with a reduction in the effect of the *Act5C-y-IR* construct in females and in fact in these flies the yellow phenotype due to the presence of the construct is not so strong (Figure 3F).

UAS-*aub* flies bearing the *Act5C-y-IR* chromosome exhibit a yellow^{+} phenotype: To confirm that the *aub* gene overexpression is the cause of the impaired RNAi process in somatic tissues, we used a UAS-*aub* strain that, subsequent to the activation by the Gal4 protein, overexpresses the *aub* gene and is able to rescue *aub* loss-of-function mutant defects (HARRIS and MACDONALD 2001). We crossed UAS-*aub* males with *Act5C-y-IR*/TM6B females to obtain individuals bearing the *Act5C-y-IR* construct in which the *aub* gene is overexpressed because of the constitutive Gal4 protein production. To compare the expression of the *aub* gene in the UAS-*aub* strain after Gal4 protein activation we performed real-time PCR experiments in these individuals. The results are shown in supplemental Tables 4 and 5 and in supplemental Figure 1S. It is clear that there is an increment of the *aub* gene transcription in *Act5C-y-IR*/UAS-*aub* individuals (supplemental Figure 1S, A, bar 2, and C, bar 2); it increases 7.5-fold in males and 7.2-fold in females with respect to UAS-*aub* individuals. The *Act5C-y-IR*/UAS-*aub* individuals showed a yellow^{+} phenotype (supplemental Figure 2S, B and E), supporting the hypothesis that the overexpression of the *aub* gene is responsible for the impaired RNAi in somatic tissues.

***aub*^{HN}/*aub*^{QC42} transheterozygous flies bearing the *Act5C-y-IR* chromosome exhibit a yellow phenotype:** To support the idea that Aub overexpression in an *aub*^{sting} mutant background is responsible for the suppression of *yellow* RNAi, we decided to look at the phenotypes of *aub*^{HN}/*aub*^{QC42} heteroallelic flies in the presence of the *Act5C-y-IR* construct. It is known that the *aub*^{HN} and *aub*^{QC42} alleles show hypomorphic phenotypes (WILSON *et al.* 1996) and in the transheterozygotes *aub*^{HN}/*aub*^{QC42} the RNAi process is impaired in germ tissues (KENNERDELL *et al.* 2002; VAGIN *et al.* 2006). To obtain flies with the genotypes of our interest we used the *Sco/CyO; MKRS/TM6B* strain to introduce dominant markers on chromosome 3 of the *aub*^{HN} strain and on chromosome 2 of the *Act5C-y-IR* strain; we crossed *aub*^{HN}/*Sco*; +/*TM6B* males with +/*CyO; Act5C-y-IR* /*MKRS* females. We recovered *aub*^{HN}/*CyO*; *Act5C-y-IR/TM6B* males and they were crossed with *aub*^{QC42}/*CyO*; +/+ females. From this cross we selected individuals that were *aub*^{HN}/*aub*^{QC42}; *Act5C-y-IR*/+ transheterozygotes. All these flies show a yellow-like phenotype as shown in supplemental Figure 3S, C and G, and for this reason we can conclude that in these flies, somatic RNAi, triggered by a hairpin *yellow* dsRNA, works. This result strongly supports our suggestion that in *aub*^{sting} homozygous flies somatic RNAi is

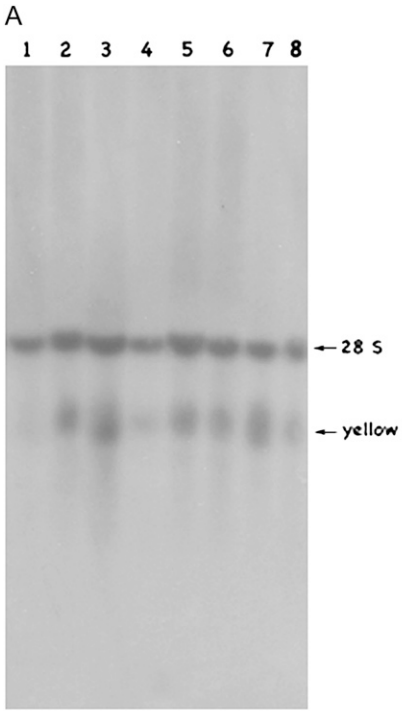

B

		Relative amount of *yellow* transcript/*28S*	Fold change
Males *Act5C-y-IR/+; +/+*	(bar1)	0,12709	0,11447
Males *+/+; aub^{sting}/aub^{sting}*	(bar2)	1,11022	1
Males *Act5C-y-IR/+; aub^{sting}/aub^{sting}*	(bar3)	1.06401	0,95837
Males *Act5C-y-IR/+; aub^{sting}/+*	(bar4)	0,45316	0,40817
Females *Act5C-y-IR/+; +/+*	(bar5)	0,82122	0,61733
Females *+/+; aub^{sting}/aub^{sting}*	(bar6)	1,33028	1
Females *Act5C-y-IR/+; aub^{sting}/aub^{sting}*	(bar7)	1,03860	0,78073
Females *Act5C-y-IR/+; aub^{sting}/+*	(bar8)	0,48101	0,36158

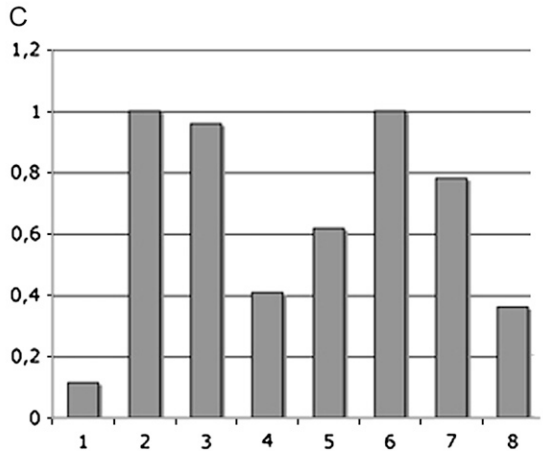

FIGURE 4.—(A) Northern blot analysis of total RNA extracted from adult individuals and hybridized with *yellow* and amplified 28S probes. Lane 1, males +/+; *Act5C-y-IR/ TM6B*; lane 2, males *aub*^{sting}*/aub*^{sting}*;* +/+; lane 3, males *aub*^{sting}*/aub*^{sting}; *Act5C-y-IR/ TM6B*; lane 4, males *aub*^{sting}*/ Sco*; *Act5C-y-IR/ TM6B*; lane 5, females +/+; *Act5C-y-IR/ TM6B*; lane 6, females *aub*^{sting}*/aub*^{sting}*;* +/+; lane 7, females *aub*^{sting}*/ aub*^{sting}; *Act5C-y-IR/ TM6B*; lane 8, females *aub*^{sting}*/ Sco*; *Act5C-y-IR/ TM6B*. (B) Densitometric values measured as (OD × millimeters × millimeters) from the Northern blot described in A. (C) Graph resulting from the relative amounts of the *yellow* transcript with respect to the 28S RNA amount, expressed on an arbitrary scale as described in the text. Bar 1, males +/+; *Act5C-y-IR/ TM6B*; bar 2, males *aub*^{sting}*/aub*^{sting}*;* +/+; bar 3, males *aub*^{sting}*/aub*^{sting}; *Act5C-y-IR/ TM6B*; bar 4, males *aub*^{sting}*/ Sco*; *Act5C-y-IR/ TM6B*; bar 5, females +/+; *Act5C-y-IR/ TM6B*; bar 6, females *aub*^{sting}*/aub*^{sting}*;* +/+; bar 7, females *aub*^{sting}*/aub*^{sting}; *Act5C-y-IR/ TM6B*; bar 8, females *aub*^{sting}*/ Sco*; *Act5C-y-IR/ TM6B*.

impaired because of the overexpression of the AUB protein.

RNAi of *yellow* transcript in *Act5C-y-IR* is impaired in somatic tissues of *aub*^{sting} mutants: To provide further support to the phenotypic analysis, we decided to analyze the expression of the *yellow* gene in all the informative genotypes. For this purpose we performed a Northern blot analysis from total RNA extracted from male and female adults in the following genotypes: (1) (+/+); *Act5C-y-IR/ TM6B*, (2) *aub*^{sting}*/aub*^{sting}*;* +/+, (3) *aub*^{sting}*/ aub*^{sting}; *Act5C-y-IR/ TM6B*, and (4) *aub*^{sting}*/ Sco*; *Act5C-y-IR/ TM6B*. We hybridized the resulting filter with *yellow* cDNA and *28S* DNA as a control. The results are shown in Figure 4A. We measured the intensity of each spot (OD × millimeters × millimeters) using the Kodak Molecular Imaging software and the relative amount of *yellow* transcript was determined by comparison with the amount of 28S RNA. All the values are reported in Figure 4B, and the related graph is shown in Figure 4C; an arbitrary value of 1 was assigned to *aub*^{sting} homozygous males (bar 2) and females (bar 6). These data suggest that *aub*^{sting} homozygotes, bearing the *Act5C-y-IR* constructs, do not show the reduction of the *yellow* transcripts that is seen in the *Act5C-y-IR*; +/+ individuals (compare bars 1 and 3 for males and bars 5 and 7 for females). This phenomenon is more evident in males than in females.

To exactly determine the amount of the *yellow* transcripts in somatic tissues, we performed a quantitative real-time PCR. We analyzed gonadless males and females of all the genotypes of our interest: (1) +/+; *Act5C-y-IR/ TM6B*, (2) *aub*^{sting}*/ aub*^{sting}*;* +/+, (3) *aub*^{sting}*/ aub*^{sting}; *Act5C-y-IR/ TM6B*, (4) *aub*^{sting}*/ Sco*; *Act5C-y-IR/ TM6B*, (5) *aub*^{HN}*/ aub*^{QC42}; *Act5C-y-IR/*+, and (6) +/+; UAS-*aub/ Act5C-y-IR*. We determined the relative amounts of *yellow* transcript with respect to the *rp49* transcript (as an internal control) for every single determination.

For all the genotypes we also calculated the CV; the results for all the determinations are reported in supplemental Tables 6 (males) and 7 (females). Hence a value of 1 was assigned to the relative amount of *yellow* with respect to the amount of *rp49* in the control genotype (*aub*^{sting}*/ aub*^{sting}*;* +/+) and the fold change for each genotype analyzed was calculated. The relative amount and the error associated with the *yellow/ rp49* estimate are shown in Figure 5. We observed a drastic reduction of *y* mRNA in *Act5C-y-IR* transgenic individuals compared to *aub*^{sting} homozygotes in both males (about 1% of expression) and females (about 30% of expression) (Figure 5A, bar 1 and Figure 5C, bar 1) confirming the phenotypic observations (Figure 3, B and F and supplemental Figure 2S). The silencing of the *yellow* gene is dramatically reduced when the genetic background of the transgenic organisms is *aub*^{sting}*/aub*^{sting}*;* +/+ and less reduced in the *aub*^{sting}*/Sco;* +/+ genotype. Individuals homozygous for the *aub*^{sting} mutation, constitutively knocked down for the *yellow* transcript, show *yellow* mRNA levels comparable to controls (*aub*^{sting}*/ aub*^{sting}; +/+), 80% for males (Figure 5A, bar 3) and 73% for females (Figure 5C, bar 3). A similar, but

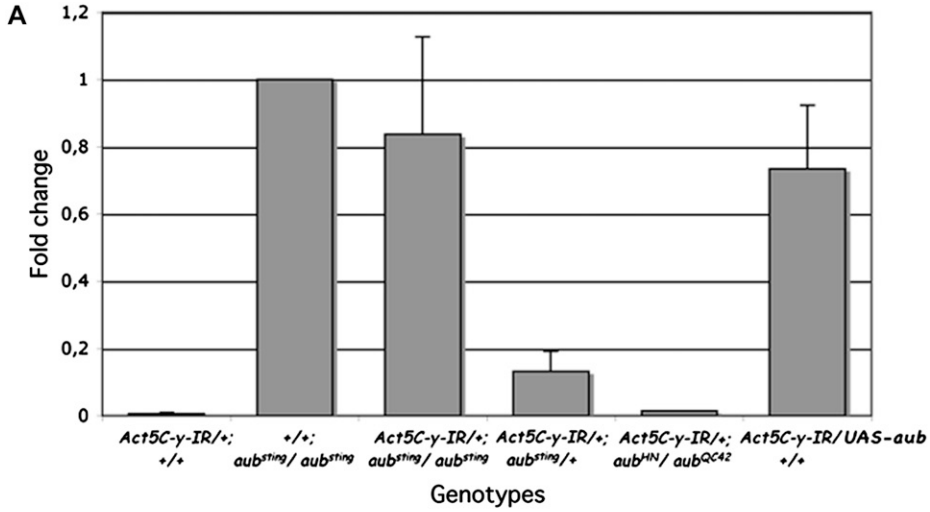

B

	Males *Act5C-y-IR/+; +/+*	Males *+/+; aub^sting/aub^sting*	Males *Act5C-y-IR/+; aub^sting/aub^sting*	Males *Act5C-y-IR/+; aub^sting/+*	Males *Act5C-y-IR/+; aub^HN/aub^QC42*	Males *Act5C-y-IR/UAS-aub +/+*
Fold change	0,006	1	0,84	0,13	0,015	0,73
Coef. of Var.	0,52	0	0,35	0,49	0,006	0,14
Stand. Dev.	0,003	0	0,3	0,064	$6,7 \times 10^{-5}$	0,2

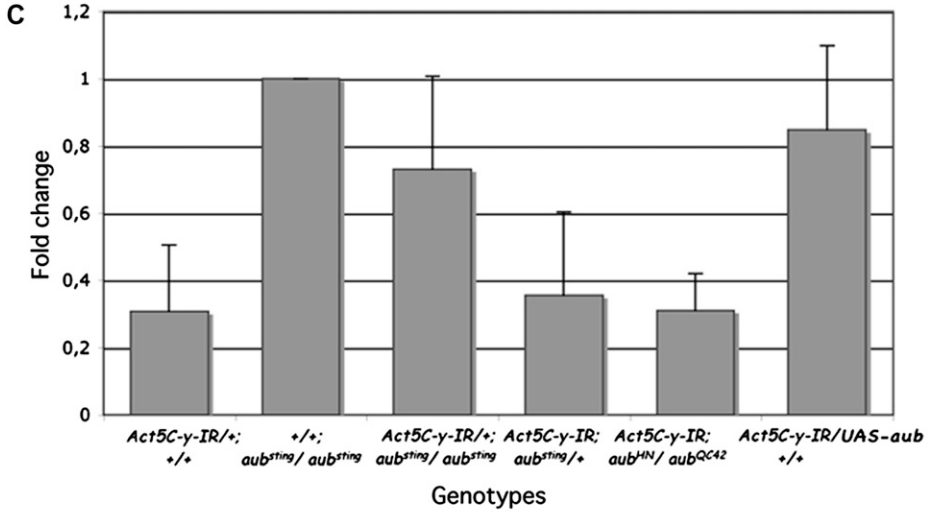

D

	Females *Act5C-y-IR/+; +/+*	Females *+/+; aub^sting/aub^sting*	Females *Act5C-y-IR/+; aub^sting/aub^sting*	Females *Act5C-y-IR/+; aub^sting/+*	Females *Act5C-y-IR/+; aub^HN/aub^QC42*	Females *Act5C-y-IR/UAS-aub +/+*
Fold change	0,31	1	0,73	0,35	0,31	0,85
Coef. of Var.	0,19	0	0,27	0,24	0,11	0,25
Stand. Dev.	0,64	0	0,37	0,70	0,35	0,21

FIGURE 5.—Real-time PCR of *yellow* transcript. Relative amounts of *yellow* transcript with respect to *rp49* in total RNA from gonadless adults are expressed on an arbitrary scale described in the text. (A) Bar 1, males +/+; *Act5C-y-IR/ TM6B*; bar 2, males *aub^sting/aub^sting;* +/+; bar 3, males *aub^sting/aub^sting*; *Act5C-y-IR/ TM6B*; bar 4, males *aub^sting/Sco*; *Act5C-y-IR/ TM6B*; bar 5, males *aub^HN/aub^QC42*; *Act5C-y-IR/ TM6B*; bar 6, males +/+; *Act5C-y-IR/UAS-aub.* (B) Fold change of *yellow* transcript of the same genotypes reported in A *vs. aub^sting/aub^sting.* (C) Bar 1, females +/+; *Act5C-y-IR/ TM6B*; bar 2, females *aub^sting/aub^sting;* +/+; bar 3, females *aub^sting/aub^sting*; *Act5C-y-IR/ TM6B*; bar 4, females *aub^sting/Sco*; *Act5C-y-IR/ TM6B*; bar 5, females *aub^HN/aub^QC42*; *Act5C-y-IR/TM6B*; bar 6, females +/+; *Act5C-y-IR/UAS-aub.* (D) Fold change of *yellow* transcript of the same genotypes reported in C *vs. aub^sting/aub^sting.*

weaker, effect can be observed in heterozygous flies *aub^sting/Sco*; +/+, 13% in males (Figure 5A, bar 4) and 35% in females (Figure 5C, bar 4). Silencing of the *yellow* gene is reduced by ~80% in somatic tissues of males and by ~43% in females, confirming the phenotypic observation (compare Figure 3, B and D, for males and Figure 3, F and H, for females). Unlike the *aub^sting* homozygotes the reduction of *yellow* silencing is not observed in the

aub^{HN}/aub^{QC42}; *Act5C-y-IR/+* individuals (supplemental Figure 3S and Figure 5, A and C, bar 5). We also demonstrated that in UAS-*aub* bearing the *Act5C-y-IR* construct, the silencing of hairpin *yellow* dsRNA is impaired as in aub^{sting} homozygotes (supplemental Figure 2S and Figure 5, A and C, bar 6).

All these results confirm that the impairing of the *yellow* silencing in somatic tissues is correlated to AUB overexpression in aub^{sting}/aub^{sting}; *Act5C-y-IR/TM6B* individuals.

DISCUSSION

In this article we have first of all analyzed the *aub* gene and protein expression in aub^{sting} mutants because we were interested in finding out whether AUB also plays a role in somatic tissues, due to the great importance that the Piwi subclade of the PPD proteins have in different RNAi pathways. Our results show that the *aub* gene is not only expressed in germ tissues, as previously reported (Schmidt *et al.* 1999), but also in male and female somatic tissues (supplemental Table 1). We also demonstrate that *aub* gene expression increases in somatic tissues of aub^{sting} homozygotes and to a lesser extent in heterozygotes; this increment is more evident in somatic tissues of males than in females (Figure 1) as previously suggested by Northern blot analyses (Schmidt *et al.* 1999). In this article we also show that the increment of the *aub* transcript in aub^{sting} homozygous mutants corresponds to an increase in the amount of AUB protein (Figure 2). Following the characterization of the $aubergine^{sting}$ mutation we used a genetic approach, based on the *Act5C-y-IR* strain, to investigate the effects of the increasing amount of AUB protein on the RNAi pathway occurring in somatic tissues *in vivo*.

The genetic experiments showed that the homozygous aub^{sting} adults bearing the *Act5C-y-IR* construct, expected to exhibit the yellow phenotype due to RNA interference, were instead phenotypically wild type (Figure 3). We obtained similar results in the genetic background bearing both the *UAS-aub* and *Act5C-y-IR* constructs (supplemental Figure 2S). In addition we performed similar crosses using a loss-of-function heteroallelic combination: aub^{HN}/aub^{QC42}; *Act5C-y-IR/+*. The results (supplemental Figure 3S) showed that somatic RNAi functions properly in this genetic background; in fact aub^{HN}/aub^{QC42}; *Act5C-y-IR/+* flies show a yellow-like phenotype. From the phenotypic analysis we proposed that the overexpression of the *aub* gene is the cause of the impaired RNAi in somatic tissue. Confirmation of the phenotypic observations came from analysis of the *yellow* transcript levels, by either Northern blot experiments or by quantitative RT–PCR (Figures 4 and 5 and supplemental Tables 6 and 7). Together these results strongly suggest that the increased amount of AUB protein observed in aub^{sting} mutants is responsible for the malfunctioning of *in vivo* RNAi, and this causes the failed transcriptional knockdown of *yellow* in the *Act5C-y-IR/+*; aub^{sting}/aub^{sting} genotype (Figure 5). We still do not have an explanation for the observed difference between the two sexes with respect to the silencing of the *yellow* gene triggered by a *yellow* dsRNA (Figure 3, B and F, and supplemental Tables 6 and 7).

How might an increased amount of AUB protein interfere with the proper functioning of RNAi in somatic tissues? A function for AUB in somatic RNAi has not been demonstrated so far; in fact a recent article showed that in Drosophila, AUB as well as PIWI are not required for hairpin-induced RNAi triggered by the *GMR-w-IR* transgene in the eye (Pelisson *et al.* 2007). From our results we could hypothesize that the increased amount of AUB somehow interferes with RISC formation in Drosophila somatic tissues. It is known that a central step in functional RISC assembly is the interaction between an ARGONAUTE protein and the small RNAs with two overhanging nucleotides at their 3′ ends; the recognition occurs by means of the PAZ domain of the AGO protein (Liu *et al.* 2004; Song *et al.* 2004; Kavi *et al.* 2005). Subsequently, in the effector step, the small unwound RNAs guide the recognition of the RNAs to be degraded and slicing occurs by means of the DDH motif of the RNase H domain of the AGO proteins (Liu *et al.* 2004; Meister *et al.* 2004; Song *et al.* 2004). In mammalian cells four Ago subfamily proteins have been identified: AGO1–AGO4. It has been reported that only AGO2 can cut the cognate mRNAs because it is the only one possessing the DDH motif in the PIWI domain that is competent for the "slicing" activity (Meister *et al.* 2004). The overexpression of AGO1, AGO3, and AGO4 interfere with the correct functioning of the RNAi pathway; in fact these proteins enter into the RISC but they are not able to slice the cognate mRNAs because they lack the DDH residues. As a matter of fact, in Drosophila it is known that the DmAGO2-containing RISC is involved in RNAi triggered by a hairpin dsRNA in somatic tissues (Lee *et al.* 2004). To test whether AUBERGINE had all the conserved amino acid residues in crucial positions of the PIWI domain we aligned the Piwi domains of four Drosophila AGO proteins: PIWI, AUB, DmAGO1, and DmAGO2. The obtained alignment, which is shown in supplemental Figure 4S, demonstrates that they have the DDH motif, which should allow them to conserve the slicing functionality. These results suggest that a different explanation should be sought for the "disturbance" caused by the overexpression of Drosophila AUB, in somatic tissues, with respect to that proposed for human cells (Meister *et al.* 2004). One alternative scenario to explain why the RNAi pathway is impaired in $aubergine^{sting}$ mutants could be as follows: by virtue of its PAZ domain, which is highly conserved in all Drosophila AGO proteins, AUB could bind the *yellow* siRNAs produced by the Dicer2/R2D2 initiator RNAi complex, subtracting them away from the competent somatic RISC and thus blocking *yellow* mRNA degradation. In

human cells, it has been demonstrated that the Piwi domain of AGO2 and the RNaseIII domain of Dicer interact directly (Doi *et al.* 2003); this interaction is mediated by the PIWI box region in the Piwi domain (Cox *et al.* 1998; Tahbaz *et al.* 2004; Lingel and Sattler 2005). The "PIWI box" of AUBERGINE appears to be slightly different, as shown in supplemental Figure 4S, from that of AGO2 which is competent for RNAi in somatic tissues leading to the suggestion that because of its different PIWI box AUB may not be able to interact with the Dicer-2/R2D2 complex and the AGO protein in the somatic RISC (Tahbaz *et al.* 2004; Lingel and Sattler 2005). Alternatively, AUB might be able to interact normally only with specific cofactors which are expressed in germ and not in somatic tissues. If this were the case, an AUB-competent RISC can be hypothesized to function specifically in germ tissues. Interestingly, AUB was thought to have a major role in silencing repetitive elements at the germ-tissue level (Vagin *et al.* 2006; Brennecke *et al.* 2007; Nishida *et al.* 2007). In addition it has been recently demonstrated that the defects in polarization of the embryo in *aub* loss-of-function mutants are suppressed by mutations in genes coding for ATR and CHK2 kinases involved in double-strand-break signaling. This suggests that the rasiRNA pathway could not be involved in axis specification but only in suppressing DNA damage signaling in the germ line (Chen *et al.* 2007; Klattenhoff *et al.* 2007). Our results support the idea that the Argonaute proteins are not interchangeable but that they have very specific roles in different RNAi pathways functioning in different tissues, at different times and in different physiological pathways.

It is becoming clear that each Piwi subclade protein binds a specific class of small interfering RNAs (piRNAs and/or rasiRNAs); Drosophila AUB and PIWI preferentially bind the antisense strands whereas AGO3 preferentially binds the sense strands of the rasi/piRNAs. Despite their differences in size and in the RNA strand involved in the binding with the PIWI proteins (rasi/piRNAs isolated from different complexes are similar from the point of view of the type of genomic elements to which they correspond) these sequences are mainly transposons (Vagin *et al.* 2006; Brennecke *et al.* 2007; Gunawardane *et al.* 2007; Lin 2007). An increased amount of the AUB proteins did impair the *Stellate* silencing *in vivo* but could not interfere with the *in vitro* production of small RNAs (siRNAs) in testicular extracts (Vagin *et al.* 2004), because the extra AUB protein produced by aub^{sting} mutants has a normal role in testis and in fact it binds the rasi/piRNAs.

Although much still remains to be done toward the detailed comprehension of the molecular machinery involved in RNAi, our work provides useful entry points to the unraveling of the role of AUBERGINE and other Piwi subfamily proteins in the Drosophila germ line and in somatic RNAi.

We thank P. Macdonald and M. Snee for providing the UAS-GFP-*aub* strain. We also thank Serafina Massari and Sergio Pimpinelli for critical reading of the manuscript. This study was supported by a grant from the Ministero dell'Università e della Ricerca (MIUR) project: genetic and molecular characterization of RNA interference involved genes in *Drosophila melanogaster*. V.S. was supported by a grant provided by MIUR for the same project. R.C. acknowledges financial support from the European Community (the 6th Framework Project EUCLOCK no. 018741). R.C. also acknowledges grants from MIUR and the Italian Space Agency (DCMC grant).

LITERATURE CITED

Aravin, A. A., N. M. Naumova, A. V. Tulin, V. V. Vagin, Y. M. Rozovsky *et al.*, 2001 Double stranded RNA-mediated silencing of genomic tandem repeats and transponsable elements in the *Drosophila melanogaster* germline. Curr. Biol. **11:** 1017–1027.

Aravin, A., M. Lagos-Quintana, A. Yalcin, M. Zavolan, D. Marks *et al.*, 2003 The small RNA profile during *Drosophila melanogaster* development. Dev. Cell **5:** 337–350.

Aravin, A., D. Gaidatzis, S. Pfeffer, M. Lagos-Quintana and P. Landgraf, 2006 A novel class of small RNAs bind to MILI protein in mouse testes. Nature **442:** 203–207.

Bier, E., H. Vaessin, S. Shepherd, K. Lee, K. McCall *et al.*, 1989 Searching for pattern and mutation in the *Drosophila* genome with a P-lacZ vector. Genes Dev. **3:** 1273–1287.

Brennecke, J., A. A. Aravin, A. Stark, M. Dus, M. Kellis *et al.*, 2007 Discrete small RNA-generating loci as master regulators of transposon activity in *Drosophila*. Cell **128:** 1089–1103.

Carmell, M. A., Z. Xuan, M. Q. Zhang and G. J. Hannon, 2002 The Argonaute family: tentacles that reach into RNAi, developmental control, stem cell maintenance, and tumorigenesis. Genes Dev. **16:** 2733–2742.

Carthew, R. W., 2006 Molecular biology. A new RNA dimension to genome control. Science **313:** 305–306.

Catalanotto, C., G. Azzalin, G. Macino and C. Cogoni, 2002 Involvement of small RNAs and role of the qde genes in the silencing pathway in Neurospora. Genes Dev. **16:** 790795.

Caudy, A. A., M. Myers, G. J. Hannon and S. M. Hammond, 2002 Fragile X-related protein and VIG associate with the RNA interference machinery. Genes Dev. **16:** 24912496.

Cerutti, H., and J. A. Casas-Mollano, 2006 On the origin and functions of RNA-mediated silencing: from protists to man. Curr. Genet. **50:** 81–99.

Cerutti, L., N. Mian and A. Bateman, 2000 Domains in gene silencing and cell differentiation proteins: the novel PAZ domain and redefinition of the Piwi domain. Trends Biochem. Sci. **25:** 481–482.

Chen, Y., A. Pane and T. Schüpbach, 2007 *cutoff* and *aubergine* mutations result in retrotransposon upregulation anc checkpoint activation in *Drosophila*. Curr. Biol. **17:** 637–642.

Collins, R. E., and X. Cheng, 2005 Structural domains in RNAi. FEBS Lett. **579:** 5841–5849.

Cook, H. A., B. S. Koppetsch, J. Wu and W. E. Theurkauf, 2004 The Drosophila SDE3 homolog *armitage* is required for *oskar* mRNA silencing and embryonic axis specification. Cell **116:** 817–829.

Cox, D. N., A. Chao, J. Baker, L. Chang, D. Qiao *et al.*, 1998 A novel class of evolutionarily conserved genes defined by *piwi* are essential for stem cell self-renewal. Genes Dev. **12:** 3715–3727.

Denli, A. M., and G. J. Hannon, 2003 RNAi: an ever-growing puzzle. Trends Biochem. Sci. **28:** 196–201.

Doench, J. G., C. P. Petersen and P. A. Sharp, 2003 SiRNAs can function as miRNAs. Genes Dev. **17:** 438–442.

Doi, N., S. Zenno, R. Ueda, H. Ohki-Hamazaki, K. Ui-Tei *et al.*, 2003 Short-interfering-RNA-mediated gene silencing in mammalian cells requires dicer and eIF2C translation initiation factors. Curr. Biol. **13:** 41–46.

Girard, A., R. Sachidanandam, G. J. Hannon and M. A. Carmell, 2006 A germline-specific class of small RNAs binds mammalian Piwi proteins. Nature **442:** 199–202.

Grivna, S. T., E. Beyret, Z. Wang and H. Lin, 2006 A novel class of small RNAs in mouse spermatogenic cells. Genes Dev. **20:** 1709–1714.

Gunawardane, L. S., K. Saito, K. M. Nishida, K. Miyoshi, Y. Kawamura *et al.*, 2007 A slicer-mediated mechanism for repeat-associated siRNA 5′ end formation in *Drosophila*. Science **315:** 1587–1590.

Hammond, S. M., A. A. Caudy and G. J. Hannon, 2001 Post-transcriptional gene silencing by double-stranded RNA. Nat. Rev. Genet. **2:** 110–119.

Harris, A. N., and P. M. Macdonald, 2001 *aubergine* encodes a *Drosophila* polar granule component required for pole cell formation and related to eIF2C. Development **128:** 2823–2832.

Hutvagner, G., and P. D. Zamore, 2002 RNAi: nature abhors a double-strand. Curr. Opin. Genet. Dev. **12:** 225–232.

Ishizuka, A., M. C. Siomi and H. Siomi, 2002 A Drosophila fragile X protein interacts with components of RNAi and ribosomal proteins. Genes Dev. **16:** 2497–2508.

Jaronczyk, K., J. B. Carmichael and T.C. Hobman, 2005 Exploring the functions of RNA interference pathway proteins: Some functions are more RISCy than others? Biochem. J. **387:** 561–571.

Kavi, H. H., H. R. Fernandez, W. Xie and J. A. Birchler, 2005 RNA silencing in Drosophila. FEBS Lett. **579:** 5940–5949.

Kennerdell, J. R., and R. W. Carthew, 2000 Heritable gene silencing in Drosophila using double-stranded RNA. Nat. Biotechnol. **18:** 896–898.

Kennerdell, J. R., S. Yamaguchi and R. W. Carthew, 2002 RNAi is activated during *Drosophila* oocyte maturation in a manner dependent on *aubergine* and *spindle-E*. Genes Dev. **16:** 1884–1889.

Kim, V. N., 2006 Small RNAs just got bigger: Piwi-interacting RNAs (piRNAs) in mammalian testes. Genes Dev. **20:** 1993–1997.

Klattenhoff, C., D. P. Bratu, N. McGinnis-Schultz, B. S. Koppetsch, H. Cook *et al.*, 2007 *Drosophila* rasiRNA pathway mutations disrupt embryonic axis specification through activation of an ATR/Chk2 DNA damage response. Dev. Cell **12:** 45–55.

Larionov, A., A. Krause and W. Miller, 2005 A standard curve based method for relative real time PCR data processing. BMC Bioinformatics **6:** 62–78.

Lee, Y. S., K. Nakahara, J. W. Pham, K. Kim, Z. He *et al.*, 2004 Distinct roles for *Drosophila* Dicer-1 and Dicer-2 in the siRNA/miRNA silencing pathways. Cell **117:** 69–81.

Lee, S. R., and K. Collins, 2006 Two classes of endogenous small RNAs in *Tetrahymena thermophila*. Genes Dev. **20:** 28–33.

Lin, H., 2007 piRNAs in the germline. Science **316:** 397.

Lindsley, D. L., and G. G. Zimm, 1992 *The Genome of Drosophila*. Academic Press, San Diego.

Lingel, A., and M. Sattler, 2005 Novel modes of protein-RNA recognition in the RNAi pathway. Curr. Opin. Struct. Biol. **15:** 107–115.

Liu, Q., T. A. Rand, S. Kalidas, F. Du, H. E. Kim *et al.*, 2003 R2D2, a bridge between the initiation and effector steps of the Drosophila RNAi pathway. Science **301:** 1921–1925.

Liu, J., M. A. Carmell, F. V. Rivas, C. G. Marsden, J. M. Thomson *et al.*, 2004 Argonaute2 is the catalytic engine of mammalian RNAi. Science **305:** 1437–1441.

Livak, K. J., and T. D. Schmittingen, 2001 Analysis of relative gene expression data using real-time quantitative PCR and the 2[-Delta Delta C(T)]. Methods **25:** 402.

Matzke, M. A., and J. A. Birchler, 2005 RNAi-mediated pathways in the nucleus. Nat. Rev. Genet. **6:** 24–35.

Meister, G., and T. Tuschl, 2004 Mechanisms of gene silencing by double-stranded RNA. Nature **431:** 343–349.

Meister, G., M. Landthaler, A. Patkaniowska, Y. Dorsett, G. Teng *et al.*, 2004 Human Argonaute2 mediates RNA cleavage targeted by miRNAs and siRNAs. Mol. Cell **15:** 185–197.

Morel, J. B., C. Godon, P. Mourrain, C. Beclin, S. Boutet *et al.*, 2002 Fertile hypomorphic ARGONAUTE (*ago1*) mutants impaired in post-transcriptional gene silencing and virus resistance. Plant Cell **13:** 629–639.

Mourelatos, Z., J. Dostie, S. Paushkin, A. Sharma, B. Charroux *et al.*, 2002 miRNPs: a novel class of ribonucleoproteins containing numerous microRNAs. Genes Dev. **16:** 720–728.

Nishida, K., K. Saito, T. Mori, Y. Kawamura, T. Nagami-Okada *et al.*, 2007 Gene silencing mechanisms mediated by Aubergine–piRNA complexes in Drosophila male gonad. RNA **13:** 1911–1922.

Okamura, K., A. Ishizuka, H. Siomi and M. C. Siomi, 2004 Distinct roles for Argonaute proteins in small RNA-directed RNA cleavage pathways. Genes Dev. **18:** 1655–1666.

Pal-Bhadra, M., U. Bhadra and J. A. Birchler, 2002 RNAi related mechanisms affect both transcriptional and posttranscriptional transgene silencing in Drosophila. Mol. Cell **9:** 315–327.

Pal-Bhadra, M., B. A. Leibovitch, S. G. Gandhi, M. Rao, U. Bhadra *et al.*, 2004 Heterochromatic silencing and HP1 localization in *Drosophila* are dependent on the RNAi machinery. Science **303:** 669–672

Pelisson, A., E. Sarot, G. Payen-Groschene and A. Bucheton, 2007 A novel repeat-associated small interfering RNA-mediated silencing pathway downregulates complementary sense gypsy transcripts in somatic cells of the Drosophila ovary. J. Virol. **4:** 1951–1960.

Pham, J. W., J. L. Pellino, Y. S. Lee, R. W. Carthew and E. J. Sontheimer, 2004 A Dicer-2-dependent 80s complex cleaves targeted mRNAs during RNAi in Drosophila. Cell **117:** 83–94.

Pham, J. W., and E. J. Sontheimer, 2005 Molecular requirements for RNA-induced silencing complex assembly in the Drosophila RNA interference pathway. J. Biol. Chem. **280:** 39278–39283.

Piccin, A., A. Salameh, C. Benna, F. Sandrelli, G. Mazzotta *et al.* 2001 Efficient and heritable functional knock-out of an adult phenotype in *Drosophila* using a GAL4-driven hairpin RNA incorporating a heterologous spacer. Nucleic Acids Res. **29:** 12e55.

Ponchel, F., C. Toomes, K. Bransfield, F. T. Leong, S. H. Douglas *et al.*, 2003 Real-time PCR based on SYBR-Green I fluorescence: an alternative to the TaqMan assay for a relative quantification of gene rearrangements, gene amplifications and micro gene deletions. BMC Biotechnol. **3:** 18–31.

Roberts, D. B., and G. N. Standen, 1998 *Drosophila: A Practical Approach*, Ed. 2. IRL, Oxford.

Saito, K., K. M. Nishida, T. Mori, Y. Kawamura, K. Miyoshi *et al.*, 2006 Specific association of Piwi with rasiRNAs derived from retrotransposon and heterochromatic regions in the Drosophila genome. Genes Dev. **20:** 2214–2222.

Sambrook, J., E. F. Fritsch and T. Maniatis, 1989 *Molecular Cloning: A Laboratory Manual*. Cold Spring Harbor Laboratory Press, Cold Spring Harbor, NY.

Schmidt, A., G. Palumbo, M. P. Bozzetti, P. Tritto, S. Pimpinelli *et al.*, 1999 Genetic and molecular characterization of *sting*, a gene involved in crystal formation and meiotic drive in the male germ line of *Drosophila melanogaster*. Genetics **151:** 749–760.

Schüpbach, T., and E. Wieschaus, 1991 Female sterile mutation on the second chromosome of *Drosophila melanogaster*. Genetics **129:** 1119–1136.

Song, J. J., S. K. Smith, G. J. Hannon and L. Joshua-Tor, 2004 Crystal structure of Argonaute and its implications for RISC slicer activity. Science **305:** 1434–1437.

St Johnston, D., and C. Nüsslein-Volhard, 1992 The origin of pattern and polarity in the Drosophila embryo. Cell **68:** 201–219.

Tahbaz, N., F. A. Kolb, H. Zhang, K. Jaronczyk, W. Filipowicz *et al.*, 2004 Characterization of the interactions between mammalian PAZ PIWI domain proteins and Dicer. EMBO Rep. **5:** 189–194.

Tang, G., 2005 siRNA and miRNA: an insight into RISCs. Trends Biochem. Sci. **30:** 106–114.

Tomari, Y., T. Du, B. Haley, D. S. Schwarz, R. Bennett, 2004 RISC assembly defects in the Drosophila RNAi mutant armitage. Cell **116:** 831–841.

Tomari, Y., and P. Zamore, 2005 Perspective: machines for RNAi. Genes Dev. **19:** 517–529.

Tritto, P., V. Specchia, L. Fanti, M. Berloco, R. D'Alessandro *et al.*, 2003 Structure, regulation and evolution of the *crystal-Stellate* system. Genetica **117:** 247–257.

Vagin, V. V., M. S. Klenov, A. I. Kalmykova, A. D. Stolyarenko, R. N. Kotelnikov *et al.*, 2004 The RNA interference proteins and vasa locus are involved in the silencing of retrotransposons in the female germ line of Drosophila melanogaster. RNA Biol. **1:** 54–58.

Vagin, V. V., A. Sigova, C. Li, H. Seitz, V. Gvozdev *et al.*, 2006 A distinct small RNA pathway silences selfish genetic elements in the germ line. Science **212:** 330–334.

Valencia-Sanchez, M. A., J. Liu, G. J. Hannon and R. Parker, 2006 Control of translation and mRNA degradation by miRNAs and siRNAs. Genes Dev. **20:** 515–524.

Vaucheret, H., 2006 Post-transcriptional small RNA pathways in plants: mechanisms and regulations. Genes Dev. **20:** 759–771.

Verdel, A., S. Jia, S. Gerber, T. Sugiyama, S. Gygi *et al.*, 2004 RNAi-mediated targeting of heterochromatin by the RITS complex. Science **303:** 672–676.

Watanabe, T., A. Takeda, T. Tsukiyama, K. Mise, T. Okuno *et al.*, 2006 Identification and characterization of two novel classes of small RNAs in the mouse germline: retrotransposon-derived siRNAs in oocytes and germline small RNAs in testes. Genes Dev. **20:** 1732–1743.

Williams, R. W., and G. M. Rubin, 2002 Argonaute1 is required for efficient RNA interference in *Drosophila* embryos. Proc. Nat. Acad. Sci. USA **99:** 6889–6894.

Wilson, J. E., J. E. Connell and P. M. Macdonald, 1996 *aubergine* enhances *oskar* translation in the *Drosophila* ovary. Development **122:** 1631–1639.

Yigit, E., P. J. Batista, Y. Bei, K. M. Pang, C. G. Chen *et al.*, 2006 Analysis of the C. elegans Argonaute family reveals that distinct Argonautes act sequentially during RNAi. Cell **127:** 747–757.

Zeng, Y., R. Yi and B. R. Cullen, 2003 MicroRNAs and small interfering RNAs can inhibit mRNA expression by similar mechanisms. Proc. Natl. Acad. Sci. USA **100:** 9779–9784.

Communicating editor: K. Golic